Neutron scattering study of spin waves in the amorphous metallic ferromagnet $(Fe_{93}Mo_7)_{80}B_{10}P_{10}$

J. D. Axe and G. Shirane
Brookhaven National Laboratory, Upton, New York 11973*

T. Mizoguchi†
IBM Research Center, Yorktown Heights, New York 10598

K. Yamauchi
Faculty of Science, Gakushuin University, Mejiro, Tokyo, Japan
(Received 9 November 1976)

Low-angle inelastic-neutron-scattering experiments were performed on an amorphous ferromagnet of composition $(Fe_{93}Mo_7)_{80}B_{10}P_{10}$ with $T_c = 450$ K. Well-defined spin waves were observed over the entire range of momentum transfer for which the scattering triangle could be closed ($q \leq 0.25$ Å^{-1}). The results were consistent with a normal ferromagnetic dispersion relation $\hbar\omega(q) = \Delta + Dq^2 + Eq^4 + \ldots$, where the gap Δ can be largely accounted for by demagnetization effects. Low-temperature magnetization measurements were performed and fit to the relation $M(T) = M_0\,(1 - BT^{3/2} - CT^{5/2})$. The measured long-wavelength spin waves account for only 70% of the density of magnon states necessary to explain $M(T)$. For temperatures below 300 K, the mean spin-wave energies are well represented by the relation $\langle\omega(q, T)\rangle = \langle\omega(q,0)\rangle[1 - 0.612(T/T_c)^{5/2}]$.

I. INTRODUCTION

Recent years have witnessed a growing interest in the phenomenon of amorphous ferromagnetism. This interest arises partly from technological considerations and partly in the hope of exposing novel and interesting physics. In some sense amorphous systems serve as a bridge between the liquid and crystalline state and this may be particularly true in the area of dynamics, where at least on a phenomenological level spin waves in ordered crystalline systems are well understood. Ultimately, we would like to achieve a comparable understanding of the spin excitations in amorphous ferromagnets. This study of the properties of relatively long wavelength spin excitation in an amorphous metal alloy by neutron scattering is one tentative step in this direction.

It is obvious by analogy with sound propagation in an amorphous elastic medium that one might expect well-defined propagating spin excitations in amorphous magnets at sufficiently long wavelengths. This was first pointed out by Kittel[1] in connection with macroscopic spin-wave theory well before amorphous magnets were discovered. It was therefore somewhat disconcerting that the first inelastic-neutron-scattering studies of amorphous metallic ferrimagnets by Pickart *et al.*[2] of composition $TbFe_2$ revealed only broad, relatively featureless magnetic scattering rather than sharp spin-wave excitations. The first inelastic-neutron-scattering experiments confirming the existence of sharp long-wavelength spin waves were those of Axe *et al.*[3] on an amorphous ferromagnet with composition $Fe_{75}P_{15}C_{10}$ and of Mook *et al.*[4] on the closely related alloy $Co_{80}P_{20}$. All of these amorphous alloys are thought to have a structure that is reasonably well described as a random dense packing of spheres,[5] which is stabilized by the appropriately different sizes of the constituent atoms in the alloys. It is now widely believed that failure to observe spin waves in the rare-earth–iron systems is connected with random single-ion anisotropy effects which are largely absent in the transition-metal–metalloid systems.

There is one very important technical difference between the neutron scattering measurements on amorphous spin waves and those in crystalline systems. It is customary in the latter case to perform experiments at a fixed momentum transfer $\vec{Q} = \vec{G} + \vec{q}$, where $\vec{G}$ is a reciprocal-lattice vector. This allows spin waves with small propagation vectors $\vec{q}$ to be observed at conveniently large scattering angles. This option is not available in an amorphous material where all wave vectors are referenced to the origin of reciprocal space, so that small $\vec{q}$ implies small scattering angles. The most fundamental of the ensuing difficulties is in the scattering kinematics which makes it impossible to transfer more than a small fraction of the incident neutron energy while maintaining the necessarily small momentum transfer. All of the transition-metal–metalloid amorphous ferromagnets mentioned in the preceding paragraph are magnetically rather stiff (e.g., the spin-wave stiffness constant $D \sim 150$ meV Å^2 for $Fe_{75}P_{15}C_{10}$, more than half of that of pure bcc Fe, $D \sim 280$ meV Å^2).[5,6] Therefore the incident neutron energy

necessary to close the scattering triangle as the spin-wave energy (or wave vector) increases is quickly driven beyond the peak of the reactor spectrum. This severely limits both the sensitivity and resolution of the experiments.

It was primarily in the hope of extending the range of the initial measurements by choosing less magnetically stiff materials that the present samples were prepared and studied. In Sec. II, we discuss sample preparation and characterization as well as the measurement of the temperature dependence of the spontaneous magnetization and the neutron scattering measurements. In Sec. III, we discuss the results of the spin-wave dispersion, the renormalization of the spin-wave energies with temperature, and the temperature-dependent spin-wave linewidth.

II. SAMPLE PREPARATION AND MEASUREMENT

An amorphous $(Fe_{93}Mo_7)_{80}B_{10}P_{10}$ alloy was prepared by rapid quenching from the melt. The resulting foils were ~25 mm in diameter and 70 μm thick. Details of the sample preparation method were the same as described elsewhere.[7] Isotope ^{11}B was used for our sample because natural boron contains about 19% of ^{10}B, which has extraordinarily high absorption for thermal neutrons.

The magnetization measurements were done with a vibrating sample magnetometer (Princeton Applied Research, model 155). No field dependence of the saturation magnetization was observed for the field above 12 kOe at 4.2 K. The temperature dependence of the magnetization was measured in the field of 12 kOe with slowly varying temperature from 4.2 to 280 K.

The neutron scattering experiments were performed using a conventional triple-axis spectrometer in the "constant-Q" mode at the Brookhaven High-Flux Beam Reactor. A stack of ~30 foils was encapsulated in a thin aluminum "pill box" filled with He gas to promote thermal conductivity and was then attached to the cold finger of a variable temperature cryostat capable of regulation to ~0.2 K or better. The foils were positioned with their faces perpendicular to the incident neutron beam. Because of the unusually small scattering angles ($2\Theta_s$ between ~0.5° and 2.0°) it was very important to minimize spurious low-angle scattering, and in particular it was helpful to reduce the thickness of the aluminum cryostat windows and it was crucial to position the pyrolytic graphite filters used to remove order contamination from the incident beam as far as possible upstream of the sample. For reasons discussed above, only a small range of energy-momentum space could be scanned with a given incident neutron energy, and various spectrometer configurations, summarized in Table I, were used to cover the range $0.06\ \text{Å}^{-1} < Q < 0.25\ \text{Å}^{-1}$ and $|\Delta E| \leq 6.2$ meV. At 14 meV, using (002) pyrolytic graphite monochromators, reasonably intense signals were obtained and the temperature dependence of the spin waves was systematically investigated in 25-K intervals from 25 to 300 K. The data taken with higher neutron energies used (002) Be monochromators, were much weaker, and were limited to a single temperature, 100 K.

Typical low-temperature, small-Q data are shown in Fig. 1. There is a substantial amount of elastic scattering, but it is nearly temperature independent and can be almost wholly accounted for by background scattering (including the cryostat and an identical empty sample cell). The cross hatching indicates the extremes of the scan dictated by the approach of the scattering angle $2\Theta_s$ to zero accompanied by a rapid rise in the background counting rate. To those with some familiarity with triple-axis spectrometry it is initially surprising that both energy gain and energy loss peaks appear equally sharp, since in general the spectrometer resolution function distorts the spectra in such a way that only one of the two peaks is "focused" in any given scan. One of the pleasant peculiarities of small-angle scattering is that the focusing is symmetric in the limit $2\Theta_s \to 0$.[8]

Figure 2 shows an example of the changes ob-

TABLE I. Summary of neutron scattering measurements at 100 K.

Q (Å^{-1})	Incident energy (meV)	Collimation (deg arc)	ΔE_{res} (meV)	$\hbar\omega_{obs}$ (meV)	$(\hbar\omega_{obs} - \Delta)/Q^2$ (meV Å^2)
0.06	14	20-10-10-10	0.3	0.342(8)	85.3(2.2)
0.08	14	...	...	0.587(3)	86.3(0.8)
0.10	14	...	...	0.885(10)	85.0(1.0)
0.15	41	20-20-20-20	0.6	1.84(10)	80.2(4.4)
0.20	60	20-10-10-20	1.0	3.23(8)	79.9(2.0)
0.25	80	...	1.0	5.11(7)	81.2(1.2)

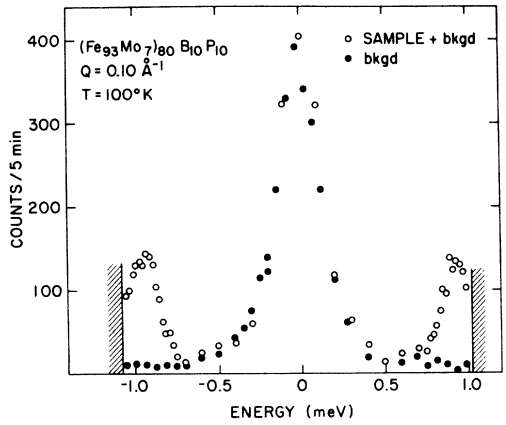

FIG. 1. Typical neutron scattering data. The elastic peak is accounted for by background from the container and cryostat. The limits of the scan (see text) are indicated by cross hatching.

served in the small-Q data over the range of temperatures studied. Since for this scan $kT \gg \hbar\omega$, the thermal occupation factor $n(\omega)$ is proportional to T and the data at the two temperatures have been scaled accordingly for ease of comparison. The data for positive and negative energy transfer at each temperature have been superimposed and are in good agreement. The renormalization of the mean spin-wave energy with increasing temperature is readily apparent. Although it is less conspicuous, there is also a gradual broadening of the spin-wave peak at temperatures above ~150 K. As will be established below, the width below this temperature can be accounted for by instrumental broadening alone.

As is well known, it is essential to correct the data for the influence of instrumental resolution.

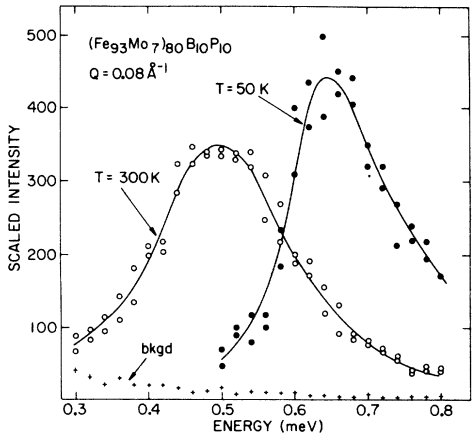

FIG. 2. Example of changes in spin-wave position and line shape with temperature. The intensities have been scaled for this comparison.

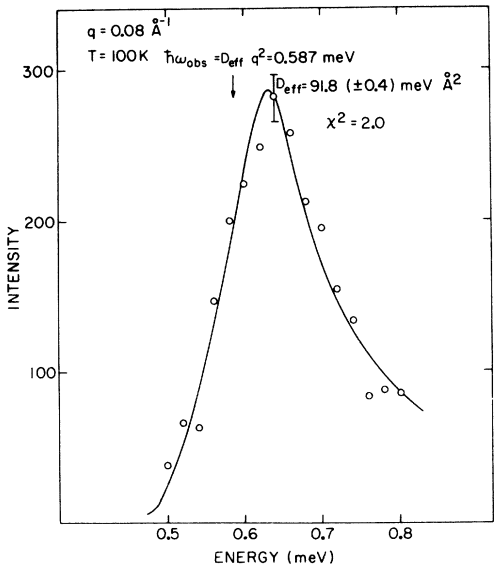

FIG. 3. Example of least squares fitting of dispersion relation convoluted with the appropriate spectrometer resolution function to observed spin-wave scattering. The arrow indicates the shift in energy due to finite resolution.

This was done by numerically convoluting the known spectrometer resolution function with a trial spin-wave dispersion relation, $\hbar\omega_{obs} = D_{eff}Q^2$, and iteratively adjusting D_{eff} to agree in the least-squares sense with the data (corrected for background). As a typical example shown in Fig. 3 demonstrates, this procedure produces satisfactory agreement at low temperatures. The calculated line shapes were systematically too narrow to account for the data above $T \approx 150$ K, which we

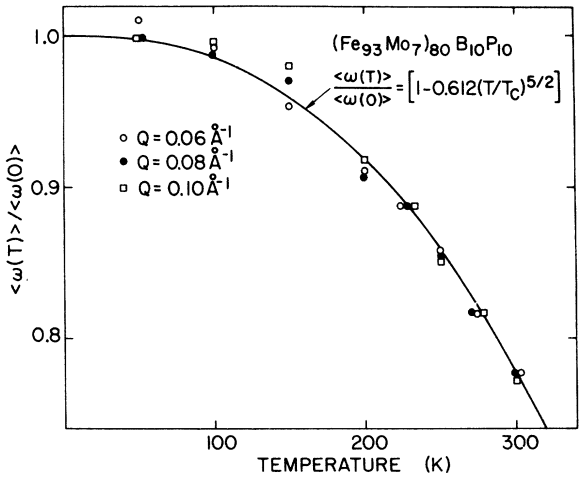

FIG. 4. Temperature dependence of the mean observed spin-wave energy for several values of momentum transfer Q.

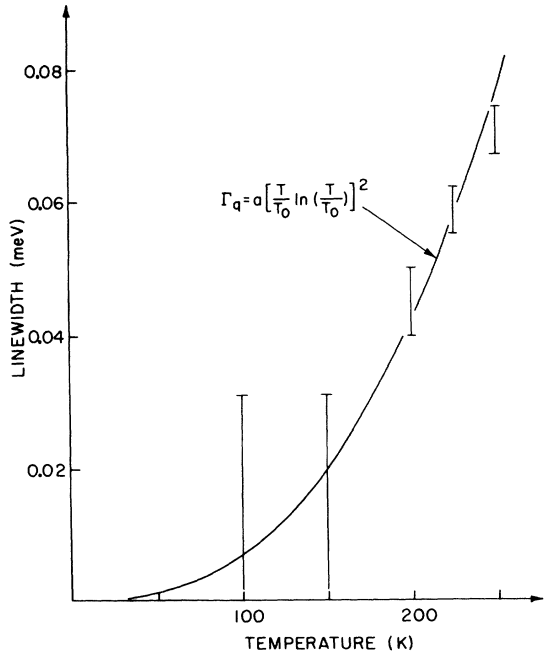

FIG. 5. Temperature dependence of the spin-wave linewidth (see text) for $Q = 0.08$ Å^{-1}.

take as evidence of intrinsic *thermal* broadening. The mean spin-wave energy is greater than the $D_{\text{eff}}Q^2$ principally by virtue of the fact that vertical resolution effects make the mean value of Q greater than the nominal value at which the center of the resolution function is positioned.

In studying the temperature-dependent renormalization of the spin-wave energies and linewidths, we chose to use the first and second frequency moments of the observed data directly rather than a least-square-fitting procedure, since particularly at high temperatures the observed line shapes were too wide to be adequately fit by our fitting routine, which assumed no intrinsic spin-wave linewidths. The data for the first moment, $\langle\omega_q(T)\rangle$, normalized to facilitate a comparison of the data taken at different Q are shown in Fig. 4. The second moment of the spin-wave profiles is considerably less accurately determined. We therefore chose to present the data for only one value of momentum transfer ($Q = 0.08$ Å^{-1}) where the scatter was smallest. At low temperatures, the width is entirely or predominantly instrumental, as we show in Fig. 3. Therefore, we show in Fig. 5 the square root of the excess second moment $\Gamma_q(T) = [\langle\omega_q^2(T)\rangle - \langle\omega_q^2(0)\rangle]^{1/2}$, where $\langle\omega_q^2(0)\rangle = 0.0070(\pm 5)$ meV^2 was calculated from the computer fit shown in Fig. 3. Assuming that the instrumental and intrinsic contributions to $\langle\omega_q^2(T)\rangle$ add in quadrature, this quantity is proportional to the intrinsic spin-wave linewidth.

III. RESULTS AND DISCUSSION

As shown in Fig. 6 (filled circles), the spin-wave dispersion data corrected for instrumental resolution, $\hbar\omega_{\text{obs}}/q^2$, display approximately the q^2 dependence expected for crystalline ferromagnets. There is, however, in the 14-meV data (the three points at lowest q) a pronounced tendency of the effective stiffness constant $\hbar\omega_{\text{obs}}/q^2$ to decrease with increasing q. These data taken alone suggest a very large q^4 correction to the spin-wave dispersion, and an extrapolated stiffness as $q \to 0$ of ~98 meV Å^2. In fact, both of these inferences were made in a preliminary account of this work.[9] This was prior to the measurements at larger momentum transfer, which make clear that a q^4 correction is not adequate. The correct explanation of the behavior of the data in Fig. 4 is the presence of a gap in the spin-wave dispersion relation at $Q = 0$, i.e.,

$$\hbar\omega(q) = \Delta + Dq^2 + Eq^4 + \ldots . \tag{1}$$

Crystalline anisotropy terms are absent in amorphous ferromagnets by symmetry, so we look elsewhere for the source of a spin-wave gap Δ. There are in general two related effects. Separating the magnetization into a static average value $\vec{M}_0$ and a time-dependent fluctuation $\delta\vec{M}(t)$, the first effect is an addition torque on the precessing magnetization equal to $-\delta\vec{M}(t) \times \vec{H}_{\text{demag}}$, where $\vec{H}_{\text{demag}} = -N_Z\vec{M}_0$ is the shape-dependent demagnetizing field. The second torque is $-\vec{M}_0 \times \delta\vec{H}(t)$, where $\delta\vec{H}(t)$ is the self-field due to $\delta\vec{M}(t)$, which depends

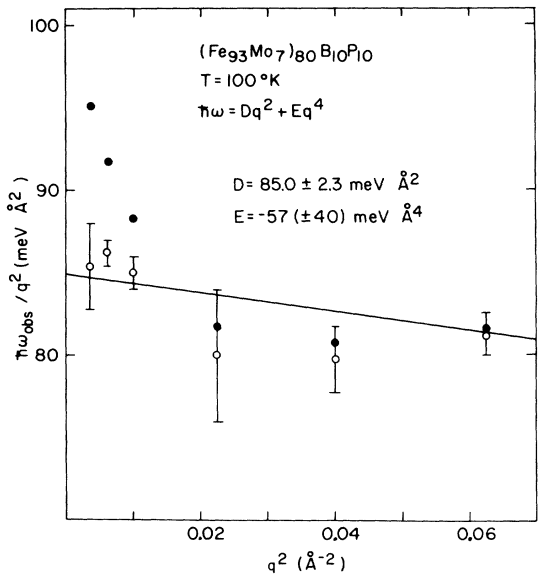

FIG. 6. Filled circles: $D_{\text{eff}} = \hbar\omega_{\text{obs}}/q^2$ vs q^2. Open circles: same data corrected for demagnetization effects (see text).

upon the relation of the propagation direction $\hat{k}$ to $\vec{M}_0$. Writing the gap for a given propagation direction in terms of an effective field $\Delta = g\mu_B H$, H is given by[10]

$$H = H_0 - [N_Z - 2\pi(1-k_Z^2)]M_0, \tag{2}$$

where H_0 is the applied external field. These effects are well known in microwave ferromagnetic resonance experiments, but are of negligible importance except at very small Q for neutron scattering. The existence of such corrections in neutron scattering was first demonstrated in Fe by Collins *et al.*[6]

In the amorphous foils in the absence of an external field, the magnetization is confined in the plane of the foil by demagnetization effects, so that $N_Z = 0$ when $H_0 = 0$. The small-angle scattering geometry also restricts $\vec{Q}$ to be nearly in the plane of the foils in our experiments, so that the average field $\langle H \rangle$ is obtained by averaging $k_{Z'}$ the projection of the unit propagation vector on $\vec{M}_0$ over the plane of the foil, weighting the average by an additional factor of $1+k_Z^2$ which occurs in the neutron scattering cross section.[11] The result is $\langle H \rangle = \frac{5}{6}\pi M_0$, and using the measured saturation magnetization $M_0 = 1154$ G and assuming $g = 2$, we find that $\langle \Delta \rangle = g\mu_B \langle H \rangle = 0.035$ meV. The last column in Table I shows the result of this correction to the measured spin-wave dispersion, as do the open circles in Fig. 6. It can be seen that this correction largely removes the anomalous dispersion at small q. Fitting the corrected data to the form suggested in Eq. (1) results in the values $D = 85.0 \pm 2.3$ meV Å^2 and $E = -57(\pm 40)$ meV Å^4 at $T = 100$ °K. Since the correction to the spin-wave energies in going from $T = 100$ to $T = 0$ °K is less than 2%, to within the uncertainties quoted we may take the values of D and E as the $T = 0$ values.

For purposes of comparison it is interesting to note that for bcc Fe Collins *et al.*[6] found $D = 281(\pm 10)$ meV Å^2 and $E = -270(\pm 35)$ meV Å^4 (at room temperature). The ratio of D/E is related to the range of the exchange interaction through $E/D = -\frac{1}{20}\langle r^2 \rangle_J$, where

$$\langle r^2 \rangle_J = \frac{\int r^2 J(r) g(r) dr}{\int J(r) g(r) dr}. \tag{3}$$

Here $J(r)$ is the range-dependent exchange interaction and $g(r)$ is the pair distribution function of the magnetic ions. The derivation, given first by Marshall[12] for a crystalline ferromagnet, can be easily generalized to the amorphous case. If in fact the ratio $|E/D| \sim 1$ Å^2 as our measurements suggest, this can, as in bcc Fe,[6] be taken as evidence of the presence of exchange interactions with a ms range, ~4 Å, which is appreciably longer than the Fe-Fe nearest-neighbor distance, which is quite sharply distributed about a mean value of ~2.5 Å.[5]

The results of the magnetization measurements are plotted vs $T^{3/2}$ in Fig. 7. At temperatures below $T \sim 150$ K, $M(T)$ is well represented by $M_0(1 - BT^{3/2})$, with $B = 5.00(\pm 0.01) \times 10^{-5}$ K$^{-3/2}$. However, over the whole temperature range a much better representation was obtained by least-squares fitting to the relation

$$M(T) = M_0(1 - BT^{3/2} - CT^{5/2}) \tag{4}$$

by adjusting the values of M_0, B, and C. The best fitting values are $M_0 = 140.0(\pm 0.1)$ emu/g (1153 G), $B = 4.5(\pm 0.2) \times 10^{-5}$ K$^{-3/2}$, and $C = 3.5(\pm 0.9) \times 10^{-8}$ K$^{-5/2}$.

As is well known[10] in conventional linear spin-wave theory, the constant B is related to the quadratic spin-wave stiffness constant D through

$$B = 2.612 \frac{g\mu_B}{M_0} \left(\frac{k_B}{4\pi D} \right)^{3/2}. \tag{5}$$

Using $D = 85.0$ meV Å^2, $g = 2.05$, and $M_0 = 1154$ G, we calculate $B = 3.12 \times 10^{-5}$ K$^{-3/2}$ or $B_{\text{calc}}/B_{\text{obs}} \sim 0.7$. Although Eq. (5) is well satisfied for bcc Fe and Ni,[10] the poor agreement found above is characteristic of the amorphous ferromagnets studied thus far by inelastic neutron scattering. For $Fe_{75}P_{15}C_{10}$, Tsuei[13] finds $B \approx 2.2 \times 10^{-5}$ K$^{-3/2}$ from low-temperature magnetization data, whereas Eq. (5) predicts $B \sim 1.3 \times 10^{-5}$ K$^{-3/2}$ using $D \sim 165$ meV Å^2 obtained from neutron scattering.[3] A discrepancy of similar magnitude seems also to exist between the measured value of B and that calculated from neutron scattering measurements using Eq. (5) for amorphous $Co_{80}P_{20}$.[13]

In conventional spin-wave theory, the term in Eq. (4) is related to the quartic corrections to the spin-wave dispersion. For isotropic spin-wave

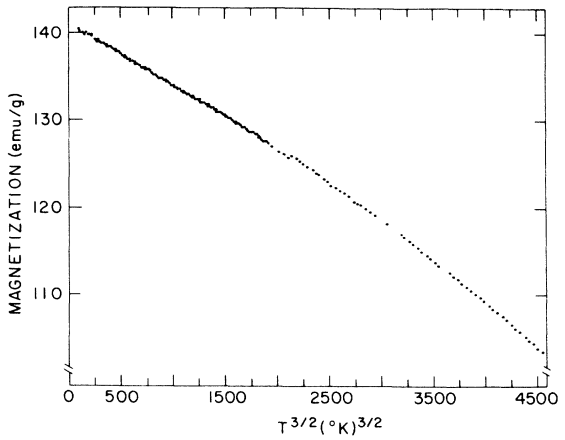

FIG. 7. Temperature dependence of sample magnetization.

dispersion the relation takes the form

$$\frac{C}{B}=\frac{3\pi}{4}\frac{\zeta(\frac{5}{2})}{\zeta(\frac{3}{2})}\frac{k}{4\pi D}\langle r^2\rangle_J .$$

Using the value $\langle r^2\rangle_J = 13.4(\pm 9.4)$ Å^2 deduced above from the ratio of E/D, we calculate $C/B = 5.0(\pm 3.5) \times 10^{-3}$ K^{-1} compared to the observed value of 0.77×10^{-3} K^{-1}. Thus there are also indications that the higher-order corrections to the magnetization renormalization cannot be accounted for in a conventional way, but in view of the uncertainty in our determination of E, this cannot be regarded as a firm conclusion.

To understand how Eq. (5) might fail for an amorphous ferromagnet it is useful to sketch out a general theoretical framework which is valid in the absence of translational symmetry.[14,15] This will also be helpful in discussing the temperature dependence of the spin-wave stiffness. For definiteness we consider Heisenberg exchange interactions of arbitrary range, $\mathcal{H}=-\sum J_{ij}S_iS_j$. Making use of the transformation to spin deviation operators $(a_i, a_i^\dagger)$, we obtain

$$S_i^+ \approx \sqrt{2s}\,a_i ,\quad S_i^- \approx \sqrt{2s}\,a_i^\dagger ,\quad S_i^z = S - a_i^\dagger a_i , \tag{6}$$

where we have dropped higher-order terms in $S_i^\pm$. The Hamiltonian becomes

$$\mathcal{H} \approx \epsilon_0 + 2S\sum J_{ij}(a_i^\dagger a_i + a_j^\dagger a_j - a_i^\dagger a_j - a_j^\dagger a_i), \tag{7}$$

where the sum is over pairs $\langle i,j\rangle$ and the ground-state energy $\epsilon_0 = 2S^2\sum J_{ij}$. Equation (7) can be diagonalized by a unitary transformation into normal mode operators $(C_\lambda, C_\lambda^\dagger)$, where $C_\lambda = \sum U_{\lambda i}a_i$, etc., so that $U = \epsilon_0 + \sum_\lambda \epsilon_\lambda n_\lambda$, where $n_\lambda = C_\lambda C_\lambda^\dagger$ is the occupation number of λth normal magnon mode with energy ϵ_λ. It is in general difficult to find the transformation matrix $U_{\lambda i}$ upon which the excitation energies depend, but in order to make contact with macroscopic or continuum spin-wave theory[1] it is necessary that we recover propagating spin waves in the long-wavelength limit, i.e., $U_{\lambda i} = N^{-1/2}e^{i\vec{q}_\lambda\cdot\vec{r}_i}$ as $\vec{q}_\lambda \to 0$. Regardless of its precise description, quantization insures that each normal mode carries one unit of spin, so that quite generally at low temperatures

$$M(T) = M_0 - \frac{g\mu_B}{V}\sum_\lambda \langle n_\lambda\rangle$$

$$= M_0 - \frac{g\mu_B}{V}\int g(\omega)n(\omega)d\omega , \tag{8}$$

where $n(\omega) = (e^{\beta\omega}-1)^{-1}$ and $g(\omega)$ is the density of magnon states. It is straightforward to show that $M(T) - M_0 \sim T^{3/2}$ implies that $g(\omega)\sim\omega^{1/2}$. Of course it is well known that the long-wavelength propagating modes with $\epsilon_\lambda \sim q_\lambda^2$ have $g(\omega)\sim\omega^{1/2}$, but the fact that $B_{\rm obs} > B_{\rm calc}$ apparently means that the spin waves contribute only ~70% (in the present case) of the low-frequency density of states. Presumably the remaining low-frequency excitations [which must also have $g(\omega)\sim\omega^{1/2}$] are more or less localized in character and do not show up in the constant-Q neutron scattering experiments which couple most strongly to plane wave excitations. It is worth noting that approximate theories of magnon densities of states for disordered and/or amorphous ferromagnets give $g(\omega)\sim\omega^{1/2}$. For example, in a study of a disordered cubic ferromagnet with random exchange, Stubbs and Montgomery[16] find that $g(\omega,\rho)\cong(1-\rho)^{-3/2}g^0(\omega)$, where ρ is a measure of the mean square deviation of J from the mean J^0, and $g^0(\omega)$ is the density of states for the ordered ferromagnet. It would be interesting to investigate theoretically whether these states are made up of both propagating and localized excitations, as the neutron scattering measurements on amorphous ferromagnets suggest.

Now consider the temperature dependence of the spin-wave energies. Keeping higher-order terms in Eq. (6) leads in a straightforward way to an improved Hamiltonian

$$U = \epsilon_0 + \sum_\lambda \epsilon_\lambda n_\lambda + \frac{1}{2}\sum_{\lambda\lambda} \epsilon_{\lambda\lambda'}n_\lambda n_{\lambda'} + \cdots \tag{9}$$

which in the Hartree approximation gives a renormalized magnon energy

$$\omega_\lambda(T) = \epsilon_\lambda + \sum_{\lambda'} \epsilon_{\lambda\lambda'}\langle n_{\lambda'}\rangle ,$$

a result first derived on more general grounds by Marshall.[11] In a cubic lattice with near-neighbor interactions Bloch[17] showed that $\epsilon_{\lambda,\lambda'}$ could be factored into $-\epsilon_\lambda\epsilon_{\lambda'}/2\epsilon_0$, so that

$$\omega_\lambda(T) = \epsilon_\lambda\left(1 - (2\epsilon_0)^{-1}\sum_{\lambda'} \epsilon_{\lambda'}\langle n_{\lambda'}\rangle\right). \tag{10}$$

Huber and Siemann[14] have recently shown that if the products of the transformation matrix $U_{\lambda i}$ which appear in $\epsilon_{\lambda\lambda'}$ for the amorphous case are replaced by certain weighted sample averages, one again recovers Eq. (10). The experimental data as plotted in Fig. 4 are in reasonable agreement with a qualitative feature of Eq. (10); namely, the fractional renormalization of all modes studied lie on a single curve.

To be more quantitative we can replace the sum in (10) by an integral over $g(\omega)$, which in turn can be evaluated in terms of the experimental magnetization renormalization constant B. The result is

$$\bar{\epsilon}=\frac{1}{V}\sum_{\lambda}\epsilon_{\lambda}\langle n_{\lambda}\rangle=\frac{1}{V}\int\omega n(\omega)g(\omega)d\omega$$

$$=\frac{3}{2}\frac{\zeta(\frac{5}{2})}{\zeta(\frac{3}{2})}\frac{M_0}{g\mu_B}BkT^{5/2}. \qquad (11)$$

The $T^{5/2}$ behavior, which follows from $g(\omega)\sim\omega^{1/2}$, is in agreement with our data as can be seen from Fig. 4 or more critically from Fig. 8. It is not possible to test Eq. (10) numerically with any accuracy without a knowledge of the ground-state energy ϵ_0. We can obtain an estimate of ϵ_0 using the results for nearest-neighbor-only exchange,[10] $2\epsilon_0/V\approx(3D/a^2)(M_0/\mu g_B)$, where a is the near-neighbor distance. Combining this with Eq. (11), Eq. (10) becomes

$$\omega_{\lambda}(T)\approx\epsilon_{\lambda}\left(1-\frac{a^2Bk}{4D}T^{5/2}\right). \qquad (12)$$

Using $a^2=2.5$ Å and measured values for B and D, we find $a^2Bk/4D=0.306T_c^{-5/2}$, which is not in particularly good agreement with the observed value of $0.612T_c^{-5/2}$. However, it is far from clear what fraction of the discrepancy is due to inaccuracy in the estimate of ϵ_0.

We know of no theories of spin-wave lifetimes formulated for amorphous ferromagnets with which to compare our linewidth results. However, in the limit $\hbar\omega_q\ll k_BT$, which holds for our measurements at high temperature, the result of a Green's-function calculation for magnon-magnon interactions in cubic lattices[18] gives for the linewidth $\Gamma(q)$

$$\Gamma(q)\propto q^4\left(\frac{T}{T_0}\ln\frac{T}{T_0}\right)^2,$$

where $T_0=\hbar\omega q/k_B$. We do not have sufficient data to test the q dependence, but the temperature dependence, while not very precisely defined by the data, seems to be consistent with this result, as shown in Fig. 5.

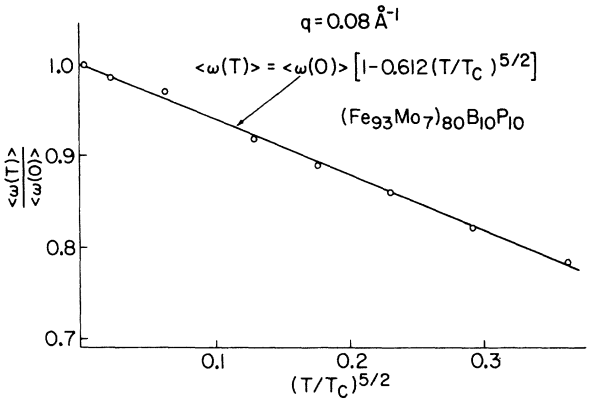

FIG. 8. Temperature dependence of mean spin-wave energy for $q=0.08$ Å^{-1}, demonstrating $T^{5/2}$ behavior.

In conclusion, our measurements confirm the existence of propagating spin waves with long lifetimes in amorphous magnets over a considerable range of wavelengths. They have (aside from demagnetization effects) a normal Dq^2 dispersion relation. At low temperatures $M_0-M(T)\sim T^{3/2}$ and $\omega_q(0)-\omega_q(T)\sim T^{5/2}$, both results consistent with a magnon density of states proportional to $\omega^{1/2}$ at low energies. However, it appears that the propagating modes seen in this study exhaust only a fraction of the density of states. This is consistent with earlier neutron scattering studies, but at variance with the recent work on amorphous $Co_{75}P_{25}$ of McColl *et al.*,[19] who found D by ferromagnetic resonance to be in agreement with that deduced from $M(T)$.

ACKNOWLEDGMENTS

It is a pleasure to acknowledge helpful conversations with R. Alben, G. S. Cargill III, J. W. Lynn, C. C. Tseui, and Y. Ishikawa.

*Work at Brookhaven performed under the auspices of the U. S. Energy Research and Development Administration.

†Permanent address: Faculty of Science, Gakushuin University, Mejiro, Tokyo, Japan.

[1]C. Kittel, J. Phys. Radium 20, 145 (1959).
[2]S. J. Pickart, J. J. Rhyne, and H. A. Alperin, Phys. Rev. Lett. 33, 424 (1974).
[3]J. D. Axe, L. Passell, and C. C. Tsuei, AIP Conf. Proc. 24, 119 (1974).
[4]H. A. Mook, D. Pan, J. D. Axe, and L. Passell, AIP Conf. Proc. 24, 112 (1974).
[5]G. S. Cargill III, in *Solid State Physics*, edited by F. Seitz, D. Turnbull, and H. Ehrenreich (Academic, New York, 1975), Vol. 30.
[6]M. F. Collins, V. J. Minkiewicz, R. Nathans, L. Passell, and G. Shirane, Phys. Rev. 179, 417 (1969).
[7]T. Mizoguchi, K. Yamauchi, and H. Miyajima, in *Amorphous Magnetism*, edited by H. O. Hooper and A. M. de Graaf (Plenum, New York, 1973), p. 325.
[8]J. Als-Nielsen and G. Shirane (private communication).
[9]J. D. Axe, AIP Conf. Proc. 29, 146 (1975).
[10]F. Keffer, in *Encyclopedia of Physics* (Springer, Berlin, 1966), Vol. XVIII-2, p. 49.
[11]See, for example, W. Marshall and S. W. Lovesey, *Theory of Thermal Neutron Scattering* (Oxford, London, 1971), p. 261.
[12]W. Marshall, in *Proceedings of the Eighth International Conference on Low-Temperature Physics* (London, 1962).

[13]C. C. Tsuei (unpublished).
[14]D. L. Huber and R. P. Siemann, Solid State Commun. 17, 769 (1975).
[15]R. Alben, AIP Conf. Proc. 29, 136 (1975).
[16]R. M. Stubbs and C. G. Montgomery, in *Amorphous Magnetism*, edited by H. O. Hooper and A. M. de Graaf (Plenum, New York, 1973), p. 413.
[17]M. Bloch, Phys. Rev. Lett. 9, 286 (1962).
[18]A. B. Harris, Phys. Rev. 175, 674 (1968); 184, 606 (1969).
[19]J. R. McColl, D. Murphy, G. S. Cargill III, and T. Mizoguchi, AIP Conf. Proc. 29, 172 (1976).